Dynamics and stability of muscle activations during walking in healthy young and older adults

Hyun Gu Kang[a,b,c,d,*] and **Jonathan B. Dingwell**[e]

[a]Institute for Aging Research, Hebrew SeniorLife, Boston MA 02131

[b]Gerontology Division, Beth Israel Deaconess Medical Center, Boston MA 02215

[c]Harvard Medical School, Boston MA 02215

[d]Department of Biomedical Engineering, Boston University, Boston MA 02215

[e]Department of Kinesiology & Health Education, University of Texas, Austin, TX 78712

Abstract

To facilitate stable walking, humans must generate appropriate motor patterns and effective corrective responses to perturbations. Yet most EMG analyses do not address the continuous nature of muscle activation dynamics over multiple strides. We compared muscle activation dynamics in young and older adults by defining a multivariate state space for muscle activity. Eighteen healthy older and 17 younger adults walked on a treadmill for 2 trials of 5 minutes each at each of 5 controlled speeds (80 – 120% of preferred). EMG linear envelopes of *v. lateralis, b. femoris, gastrocnemius*, and *t. anterior* of the left leg were obtained. Interstride variability, local dynamic stability (divergence exponents) and orbital stability (maximum Floquet multipliers; FM) were calculated. Both age groups exhibited similar preferred walking speeds ($p = 0.86$). Amplitudes and variability of individual EMG linear envelopes increased with speed ($p < 0.01$), in all muscles but *gastrocnemius*. Older adults also exhibited greater variability in *b. femoris* and *t. anterior* ($p < 0.004$). When comparing continuous multivariate EMG dynamics, older adults demonstrated greater local and orbital instability of their EMG patterns ($p < 0.01$). We also compared how muscle activation dynamics were manifested in kinematics. Local divergence exponents were strongly correlated between kinematics and EMG, independent of age and walking speed, while variability and max FM were not. These changes in EMG dynamics may be related to increased neuromotor noise associated with aging and may indicate subtle deterioration of gait function that could lead to future functional declines.

*Please address all correspondence to: Hyun Gu Kang, Ph.D., Institute for Aging Research, Hebrew SeniorLife, 1200 Center St, Boston MA 02131, Phone: 617-363-8487, Fax: 617-363-8936, Email: hyungukang@hrca.harvard.edu, Web: www.instituteforagingresearch.org/hyungukang.

Conflict of Interest Statement

The authors declare that there is no conflict of interest associated with this work.

Introduction

Falls pose serious risks to older adults (Fuller, 2000), and most falls occur during walking (Niino et al., 2000; Berg et al., 1997). Gait disorders also lead to disability in older adults (Alexander, 1996; Alexander and Goldberg, 2005). Preventing these outcomes requires a better understanding of gait dynamics. Facilitating stable walking kinematics requires generating appropriate motor patterns and effective corrective responses to perturbations. Yet how the muscle activation patterns produced by the nervous system are then reflected in the observed kinematics, or how these relationships change with aging, are not well understood.

Since muscles generate the forces that drive walking, the dynamics observed in the kinematics presumably reflect that of muscle activation patterns. However, since kinematics are much less variable than EMG patterns during gait (Winter and Yack, 1987), kinematics appear more tightly controlled than muscle activations. This could be due to inertial and damping properties of body segments that smooth individual muscle force fluctuations. Muscle activation dynamics also reflect the need to respond to perturbations and maintain stability during walking more than producing consistent kinematics. Thus, muscle activation dynamics may *not* be reflected in kinematics. Because each kinematic degree of freedom is controlled by multiple muscles, walking kinematics result from the coordination of many muscles. Therefore, one cannot meaningfully compare the dynamics of individual joint angles to those of individual muscles.

Gait dynamics evolve over multiple strides, where each stride depends (explicitly or implicitly) on multiple previous strides (Hausdorff et al., 2001). The local dynamic stability of walking kinematics have been well characterized (Dingwell and Kang, 2007; Granata and Lockhart, 2008; Kang and Dingwell, 2008a). However, EMG has not been characterized in this manner. Mean EMG patterns change with aging (Winter and Yack, 1987), function and pathology (Abel et al., 2005), and also exhibit walking speed-related changes in both amplitudes and timing (Shiavi, 1985; Shiavi et al., 1987; Chung and Giuliani, 1997). However, these studies did not quantify EMG dynamics over consecutive strides. Also, by using self-selected speeds, these studies did not adequately control for walking speed, which greatly influences gait dynamics independently of aging (Kang and Dingwell, 2008a; Kang and Dingwell, 2008b). Variability measures do not describe how EMG fluctuations change from one stride to the next, or how multiple muscles coordinate during walking. Clustering or principal component analysis methods quantify multivariate muscle activation patterns (Ivanenko et al., 2004; Jansen et al., 2003), but not across consecutive strides.

Dynamical systems come in many types, from a wide range of scientific disciplines (Strogatz, 1994). Mathematically, all of these systems can be analyzed using the same general set of tools, regardless of how their governing state variables are defined. For biomechanical kinematic data, various different state space definitions can yield similar final conclusions (Gates and Dingwell, 2009). Continuous EMG linear envelopes exhibit strongly periodic, but slightly *a*-periodic dynamics during walking, similar to those seen in walking kinematics. Thus, methods previously used to characterize the dynamic stability of walking *kinematics* can also be validly used to characterize the dynamic stability of *muscle activations* (i.e., EMG).

In this study, we measured age- and speed-related changes in interstride variability of muscle activations. We also used state-space descriptions that account for both multivariate and multi-stride dynamics. From these, local and orbital stability (Dingwell and Kang, 2007) of EMG amplitudes were quantified to describe how multiple muscles coordinate over consecutive strides. Leg muscle activations were measured in young and older adults walking at multiple controlled speeds. Thus, the effects of age were quantified independently of walking speed (Kang and Dingwell, 2008b; Kang and Dingwell, 2008a). Finally, we determined whether the

dynamics of EMG patterns during walking were reflected in the associated dynamics of walking kinematics, which we reported previously (Kang and Dingwell, 2008b; Kang and Dingwell, 2008a).

Methods

Eighteen healthy older adults (age 65–85) and 17 height-, weight-, and gender-matched young adults (age 18–28), participated after providing informed consent as approved by the local institutional review board (Table 1). We excluded those who reported recent lower extremity injuries, visible gait asymmetries or disabilities, or those who were on medications that may influence gait.

Details of data collection are presented elsewhere (Kang and Dingwell, 2008b; Kang and Dingwell, 2008a). Subjects walked on a treadmill (Desmo S model, Woodway USA, Waukesha WI) while wearing a safety harness (Protecta International, Houston TX). Each subject's preferred walking speed (PWS) was determined using an established protocol (Dingwell and Marin, 2006; Kang and Dingwell, 2008b; Kang and Dingwell, 2006), allowing treadmill acclimation. Subjects completed two 5-minute walking trials each at 5 different speeds (0.8× −1.2×PWS), with 2 minutes of in-between rest. The order of presentation was randomized while preventing two consecutive fast speed trials to avoid fatigue. All data from one young subject (not counted above), and 1 trial from one older subject were discarded due to technical problems (Table 1). A second older subject could not complete one 1.2×PWS trial, so this trial was also discarded. Subjects were instructed to look straight ahead and avoid extraneous movements. Kinematics were measured using Vicon 612 (Oxford Metrics, UK). Kinematic analyses are presented elsewhere (Kang and Dingwell, 2008b; Kang and Dingwell, 2008a).

Muscle activation patterns during walking were recorded using surface electromyography (EMG) (Delsys, Boston MA), using bipolar electrodes from 4 muscles of the left leg: *vastus lateralis* (VL), *biceps femoris* (BF), medial head of *gastrocnemius* (GA), and *tibialis anterior* (TA) according to the SENIAM conventions (Hermens et al., 2000). The EMG signals were sampled at 1080 Hz, bandpass filtered (passband 20–300 Hz), notch-filtered at 60 Hz using a Butterworth filter, and demeaned (MATLAB 7.04, Mathworks, Natick MA). Then, signals were normalized to the peak amplitude during the preferred walking speed trial of each person, to allow for better comparison between subjects. These normalized signals were then rectified, and low-pass filtered using a Hamming averaging window (bell-shaped curve) of 100 ms, equivalent to a low-pass filter with 10Hz cutoff (Granata et al., 2004). Once smoothed, the signal was down-sampled to 60Hz to determine the EMG linear envelopes used in subsequent analyses. Noisy sections of the signals due to static discharge, electrode dys-adhesion, etc. as identified via visual inspection were not used in subsequent analyses. In some subjects, the VL muscle was mostly inactive during slow walking speeds (Ivanenko et al., 2006). Such trials (15 out of 349 collected) were not included in the variability analysis for VL, because they would excessively lower the observed variability. Likewise, several individual trials for BF (17/349), GS (8/349), and TA (7/349) muscles were excluded due to poor signal quality. Any walking trials with any unusable EMG signal(s) (total 29/349) were not used in the stability analyses because the state-space could not be defined similarly as other trials.

For each trial, the data for each stride were normalized from 0 to 100% gait cycle. Means and standard deviations of EMG linear envelopes were calculated at each percentage of gait cycle. To determine the variability of each EMG linear envelope over the entire gait cycle, MeanSD's were determined (Dingwell and Marin, 2006; Dingwell and Cavanagh, 2001; Kang and Dingwell, 2008b):

$$\text{MeanSD} = \langle SD(i) \rangle_i, \; i \in \{0 - 100\% \text{ gait cycle}\} \tag{1}$$

where $SD(i)$ indicates the standard deviation of a measure at ith % gait cycle, and $\langle \; \rangle_i$ denotes the average over all i. MeanSD and average peak amplitude values were each calculated for each muscle of each trial (Figure 1).

Previous work showed that as few as 5 principal components can reconstruct most features of multiple EMG signals recorded during walking (Ivanenko et al., 2004; Ivanenko et al., 2006). This suggests that 5 or more state variables should be sufficient to describe the dynamics of the muscle activation patterns during walking. EMG dynamics were therefore described using the four normalized (now unitless) signals as processed above, as well as their time derivatives (Packard et al., 1980), which were non-dimensionalized by $\sqrt{l/g}$, where l = leg length (Hof, 1996). These defined an 8-dimensional unitless state-space (Figure 2A):

$$\mathbf{S}(t) = [\, V_1(t) \; V_2(t) \; V_3(t) \; V_4(t) \; \dot{V}_1(t) \; \dot{V}_2(t) \; \dot{V}_3(t) \; \dot{V}_4(t)\,] \in \mathfrak{R}^8 \tag{2}$$

where V is the normalized linear envelope of EMG voltage, and $\dot{V}$ corresponding time-derivative. Time derivatives of EMG signals were included to capture the rate of activation dynamics. A state-space of 8 dimensions is more than adequate to describe dynamics that occur in 5 dimensions (Ivanenko et al., 2004; Kennel et al., 1992).

The sensitivity of these multivariate EMG patterns to small inherent perturbations that naturally occur during walking were quantified in two ways. First, *local* dynamic stability (Figure 2B) was quantified (Dingwell and Cusumano, 2000; Kang and Dingwell, 2008a; England and Granata, 2007). Euclidean distances between neighboring trajectories in state space were computed as a function of time (Figure 2B) and averaged over many original pairs of initially nearest neighbors (Rosenstein et al., 1993). Local divergence exponents (λ^*) were estimated from the slopes of linear fits to these curves:

$$y(i) = \frac{1}{\Delta t} \left\langle \ln[\, d_j(i)\,] \right\rangle = [\,\lambda^*\,] i + c \tag{3}$$

where $d_j(i)$ was the Euclidean distance between the jth pair of initially nearest neighbors after i discrete time steps (*i.e.* $i\Delta t$ seconds) and $\langle \cdot \rangle$ denotes the average over all values of j (Rosenstein et al., 1993). Positive exponents indicate local instability, with larger exponents indicating greater local instability, or greater sensitivity to small perturbations. Since the intrinsic time scales (*i.e.*, average stride times) were different for each subject, the time axes of these curves were re-scaled by multiplying by the average stride frequency for each subject. Short-term exponents (λ^*_s) were calculated from the slopes of linear fits to the divergence curves between 0 and 1 stride. Long-term exponents (λ^*_L) were calculated as the slopes between 4 and 10 strides (Figure 2B) (Dingwell et al., 2000).

Second, *orbital* stability was quantified by calculating maximum Floquet Multipliers (FM) using established techniques (Hurmuzlu et al., 1996; Donelan et al., 2004). First, we defined a Poincaré section (Figure 2C) at each percentage of the gait cycle (0% to 100%), where 0% defined left heel strike. The system state $\mathbf{S}_k$ for each stride k at that Poincaré section evolved to a state at the following stride, $\mathbf{S}_{k+1}$, according to the Poincaré map (Eq. 4):

$$\mathbf{S}_{k+1} = \mathbf{F}(\mathbf{S}_k) \tag{4}$$

We defined the limit cycle trajectory as the average trajectory across all strides within a trial. This limit cycle trajectory produces a single fixed point in each Poincaré section:

$$\mathbf{S}^* = \mathbf{F}(\mathbf{S}^*) \tag{5}$$

We then computed the effects of small perturbations away from these fixed points, using a linearized approximation of Eq. (4):

$$[\mathbf{S}_{k+1} - \mathbf{S}^*] \approx J(\mathbf{S}^*)[\mathbf{S}_k - \mathbf{S}^*] \tag{6}$$

For $\mathbf{S} \in {}^8$, $J(\mathbf{S}^*) \in {}^{8 \times 8}$ had 8 eigenvalues. The first 7 eigenvalues of $J(\mathbf{S}^*)$ defined the Floquet Multipliers (FM) that quantified how much small perturbations in the Poincaré section grew or diminished by the next cycle (Kang and Dingwell, 2008a). If these FM all have magnitude < 1, perturbations on average shrink by the next stride, and the system remains stable. We computed the magnitudes of the *maximum* FM for Poincaré sections at 0%, 25%, 50%, and 75% of the gait cycle, as we did previously (Kang and Dingwell, 2008a).

EMG peak amplitudes, MeanSD's, local divergence exponents, λ^*_S, λ^*_L, and maximum FM at 0%, 25%, 50%, and 75% of the gait cycle were compared between age groups and across speeds using a general linear model analysis of variance (ANOVA) using SPSS 14 (SPSS, Chicago IL). To compare the variability and stability metrics derived from EMG and previously reported kinematics (Kang and Dingwell, 2008a), we used Pearson correlation (*r*), as well as general linear model analysis of covariance (ANCOVA) using SAS 9.1 (SAS Institute, Cary NC). ANCOVA was used to determine the correlation between kinematics– and EMG–derived stability metrics independent of the effects of age and speed. The ANCOVA model for each EMG–derived stability metric included age, speed, age×speed interaction, plus the corresponding kinematics-derived metric as a covariate.

Results

Peak EMG amplitudes increased with speed for all four muscles ($p < 0.001$). Older adults displayed higher amplitudes in *v. lateralis* (VL) ($p < 0.003$), *b. femoris* (BF) ($p < 0.001$), and *gastrocnemius* (GS) ($p < 0.03$; Figure 2). Variability (MeanSD) of EMG increased with speed in VL, BF, and *t. anterior* (TA) muscles ($p < 0.001$; Table 2). The main effect for speed was also significant for *gastronemius* ($p = 0.027$; Table 2). However, post-hoc analyses revealed that only the 0.8×PWS and 1.2×PWS speeds were different and these differences were quite small (Fig. 3). Variability was also larger in older adults in BF ($p = 0.003$) and TA ($p < 0.001$) muscles. Interaction effects were not significant. However, MeanSD of GS was not different between age groups and speed effects were marginal ($p = 0.03$).

Both divergence exponents λ^*_s and λ^*_L increased with speed ($p < 0.001$), while λ^*_s was greater in older adults ($p < 0.003$; Fig 4; Table 2). Thus the EMG amplitude pattern was more sensitive to perturbations in older adults independently of speed. Maximum FM of older adults were larger at 0, 25, 50, and 75% of the gait cycle ($p < 0.009$; Figure 5). FM did not vary significantly with speed ($p = 0.2$), but interaction effects were significant at 25% ($p < 0.001$), where speed effects were seen only in young adults (Tukey's LSD post-hoc $p < 0.003$).

Among kinematic variability results published previously (Kang and Dingwell, 2008b), sagittal plane knee flexion/extension angle MeanSD was slightly correlated with EMG MeanSD's for VL ($r^2 = 0.04$, $p < 0.001$, where r^2 is from Pearson *r*), BF ($r^2 = 0.02$, $p = 0.02$), and TA ($r^2 = 0.14$, $p < 0.001$; Fig. 6A) muscles. After accounting for age and speed in the ANCOVA model, EMG MeanSD's for VL ($R^2 = 0.03$, $p = 0.001$, where R^2 is the proportion of variance explained

by the covariate), and TA ($R^2 = 0.07$, $p < 0.001$), but not for BF ($R^2 = 0.001$, $p = 0.5$) were still significantly correlated to kinematic variability (not shown). However, these correlations were relatively weak ($r^2 \leq 0.14$; $R^2 \leq 0.07$). Ankle plantar/dorsiflexion angle MeanSD was also slightly correlated with EMG MeanSD's of VL and GS ($r^2 \leq 0.015$, $p \leq 0.026$), and in the ANCOVA model, ($R^2 = 0.014$, $p < 0.04$).

In contrast, both λ^*_s and λ^*_L derived from EMG-based and kinematics-based (Kang and Dingwell, 2008a) state spaces were strongly correlated ($r^2 = 0.49$ and 0.61; $p < 0.001$; Fig. 6). In the ANCOVA model, these relationships remained highly significant ($R^2 = 0.38$ and $R^2 = 0.52$, $p < 0.001$; Fig. 6). However, maximum FM measures were only slightly correlated between EMG and kinematics ($r^2 \leq 0.09$; $p < 0.001$), and not correlated after accounting for age and speed effects ($R^2 < 0.01$, $p = 0.41$).

Discussion

Older adults exhibited greater interstride variability of muscle activation patterns during gait (Fig. 3). However, motor system pathology affects gait timing dynamics over multiple strides (Hausdorff et al., 1997). Traditional EMG analyses fail to account for the continuous nature of muscle activation dynamics over multiple consecutive strides, or coordination across multiple muscles. By using novel state-space descriptions of multi-muscle activations over time, we found that older adults exhibit greater interstride dynamic instability of muscle activation patterns during gait (Fig. 4 & Fig 5). By comparing measures of EMG dynamics to those of kinematics (Fig. 6), we also demonstrate for the first time that multi-dimensional dynamics of muscle activations are reflected in that of kinematics, while interstride variability is not.

Variability of EMG patterns during gait increased with speed, except in the *gastrocnemius* (Fig. 3). Variability of *gastrocnemius* activation did not vary with age or speeds, perhaps because the activation of the plantarflexors is carefully managed, as these propulsive muscles (Neptune et al., 2007) add mechanical energy to the system. Age-related differences were seen only in *b. femoris* and *t. anterior*. This is unlike sagittal leg joint angles, which did not exhibit this speed or age relationship (Kang and Dingwell, 2008b), and showed only small correlations ($r^2 \leq 0.14$; $R^2 \leq 0.07$) with that of EMG. Thus, interstride variability of EMG patterns is only marginally reflected in that of kinematics. This validated the idea that comparing activation patterns of individual muscles with individual kinematic variables cannot account for the coordination and synergies of multiple muscles.

EMG patterns in older adults exhibited greater local (Fig. 4) and orbital (Fig. 5) instability, similar to their kinematics (Kang and Dingwell, 2008a). Thus, muscle activation patterns may be more easily perturbed in these older adults, which may explain the similar kinematics results. Older adults exhibit increased EMG response latencies to perturbations (Lin and Woollacott, 2002;Pijnappels et al., 2005). The increased λ^*_s and maximum FM observed during unperturbed walking likely reflect the slowed responses to perturbations.

Our state-space analyses also demonstrated that local instability of the multivariate dynamics of kinematics and EMG were strongly correlated (Fig. 6), even after accounting for age and speed differences. Thus, the local stability properties of multivariate EMG dynamics are manifested in the multivariate dynamics of kinematics. Howver, since muscle activations measured using EMG do not represent muscle *forces*, it is not yet clear how these muscle activation dynamics generate the muscle forces that lead to the observed kinematics. Dynamic simulation studies could help address these questions.

This study only included very healthy older adults. Therefore, our findings may not translate directly to understanding risk for falls. However, we found differences in muscle activation

dynamics even in healthy older adults who had no prior history of falls and who did not exhibit slower walking speeds that might otherwise indicate functional decline (Alexander, 1996). Therefore, the observed changes in muscle activation dynamics may be a precursor to *future* functional declines. Detecting these changes early may help prevent further loss of gait function. This needs to be tested in a clinical outcomes study.

The mechanisms that generate muscle activations to produce normal gait appear to give rise to state-space attractor (Nayfeh and Balachandran, 1995). These mechanisms likely involve spinal central pattern generators (Shik and Orlovsky, 1976; Ivanenko et al., 2006) and sensory feedback. These neural structures may deteriorate with aging, and thus may not be able to respond as easily to perturbations to restore normal gait. This deterioration could arise from increased neuromotor noise (Dean et al., 2007; Faisal et 2008) or randomness (Hausdorff et al., 1997) that occurs with aging, and which could alter the internal dynamics of the attractor. Deteriorated brain function associated with diminished cognitive function or motor system diseases leads to gait problems in older adults (Allali et al., 2007; Atkinson et al., 2007; Ben-Itzhak al., 2008; Holtzer et al., 2006). Future work should investigate the roles of noise in the nervous system brain function in the gait of older adults.

Acknowledgements

References

Abel MF, Damiano DL, Gilgannon M, Carmines D, Kang HG, Bennett BC, Laws ER Jr. Biomechanical Changes in Gait Following Selective Dorsal Rhizotomy. Journal of Neurosurgery 2005;102(2 Suppl): 157–162. [PubMed: 16156224]

Alexander NB. Gait Disorders in Older Adults. Journal of the American Geriatrics Society 1996;44(4): 434–451. [PubMed: 8636592]

Alexander NB, Goldberg A. Gait Disorders: Search for Multiple Causes. Cleveland Clinic Journal of Medicine 2005;72(7):586. [PubMed: 16044655]9–90, 92–4 passim

Allali G, Kressig RW, Assal F, Herrmann FR, Dubost V, Beauchet O. Changes in Gait While Backward Counting in Demented Older Adults with Frontal Lobe Dysfunction. Gait and Posture 2007;26(4): 572–576. [PubMed: 17344044]

Atkinson HH, Rosano C, Simonsick EM, Williamson JD, Davis C, Ambrosius WT, Rapp SR, Cesari M, Newman AB, Harris TB, Rubin SM, Yaffe K, Satterfield S, Kritchevsky SB. Cognitive Function, Gait Speed Decline, and Comorbidities: The Health, Aging and Body Composition Study. Journals of Gerontology. Series A, Biological Sciences and Medical Sciences 2007;62(8):844–850.

Ben-Itzhak R, Giladi N, Gruendlinger L, Hausdorff JM. A Double-Blind, Single-Dose Cross-over Study. Can Methylphenidate Reduce Fall Risk in Community-Living Older Adults? Journal of American Geriatrics Society 2008;56(4):695–700.

Berg WP, Alessio HM, Mills EM, Tong C. Circumstances and Consequences of Falls in Independent Community-Dwelling Older Adults. Age and Ageing 1997;26(4):261–268. [PubMed: 9271288]

Chung SH, Giuliani CA. Within- and between-Session Consistency of Electromyographic Temporal Patterns of Walking in Non-Disabled Older Adults. Gait and Posture 1997;6(2):110–118.

Dean JC, Alexander NB, Kuo AD. The Effect of Lateral Stabilization on Walking in Young and Old Adults. IEEE Transactions on Biomedical Engineering 2007;54(11):1919–1926. [PubMed: 18018687]

Dingwell JB, Cavanagh PR. Increased Variability of Continuous Overground Walking in Neuropathic Patients Is Only Indirectly Related to Sensory Loss. Gait and Posture 2001;14(1):1–10. [PubMed: 11378419]

Dingwell JB, Cusumano JP. Nonlinear Time Series Analysis of Normal and Pathological Human Walking. Chaos: An Interdisciplinary Journal of Nonlinear Science 2000;10(4):848–863.

Dingwell JB, Cusumano JP, Sternad D, Cavanagh PR. Slower Speeds in Neuropathic Patients Lead to Improved Local Dynamic Stability of Continuous Overground Walking. Journal of Biomechanics 2000;33(10):1269–1277. [PubMed: 10899337]

Dingwell JB, Kang HG. Differences between Local and Orbital Dynamic Stability During Human Walking. Journal of Biomechanical Engineering 2007;129(4):586–593. [PubMed: 17655480]

Dingwell JB, Marin LC. Kinematic Variability and Local Dynamic Stability of Upper Body Motions When Walking at Different Speeds. Journal of Biomechanics 2006;39(3):444–452. [PubMed: 16389084]

Donelan JM, Shipman DW, Kram R, Kuo AD. Mechanical and Metabolic Requirements for Active Lateral Stabilization in Human Walking. Journal of Biomechanics 2004;37(6):827–835. [PubMed: 15111070]

England SA, Granata KP. The Influence of Gait Speed on Local Dynamic Stability of Walking. Gait and Posture 2007;25(2):172–178. [PubMed: 16621565]

Faisal AA, Selen LP, Wolpert DM. Noise in the Nervous System. Nature Reviews Neuroscience 2008;9 (4):292–303.

Fuller GF. Falls in the Elderly. American Family Physician 2000;61(7):2173–2174.

Gates DH, Dingwell JB. Comparison of Different State Space Definitions for Local Dynamic Stability Analyses. Journal of Biomechanics. 2009in press

Granata KP, Lockhart TE. Dynamic Stability Differences in Fall-Prone and Healthy Adults. Journal of Electromyography and Kinesiology 2008;18(2):172–178. [PubMed: 17686633]

Granata KP, Slota GP, Bennett BC. Paraspinal Muscle Reflex Dynamics. Journal of Biomechanics 2004;37(2):241–247. [PubMed: 14706327]

Hausdorff JM, Ashkenazy Y, Peng CK, Ivanov PC, Stanley HE, Goldberger AL. When Human Walking Becomes Random Walking: Fractal Analysis and Modeling of Gait Rhythm Fluctuations. Physica A: Statistical Mechanics and its Applications 2001;302(1–4):138–147.

Hausdorff JM, Mitchell SL, Firtion R, Peng CK, Cudkowicz ME, Wei JY, Goldberger AL. Altered Fractal Dynamics of Gait: Reduced Stride Interval Correlations with Aging and Huntington's Disease. Journal of Applied Physiology 1997;82(1):262–269. [PubMed: 9029225]

Hermens HJ, Freriks B, Disselhorst-Klug C, Rau G. Development of Recommendations for Semg Sensors and Sensor Placement Procedures. Journal of Electromyography and Kinesiology 2000;10(5):361–374. [PubMed: 11018445]

Hof AL. Scaling Gait Data to Body Size. Gait and Posture 1996;4:222–223.

Holtzer R, Verghese J, Xue X, Lipton RB. Cognitive Processes Related to Gait Velocity: Results from the Einstein Aging Study. Neuropsychology 2006;20(2):215–223. [PubMed: 16594782]

Hurmuzlu Y, Basdogan C, Stoianovici D. Kinematics and Dynamic Stability of the Locomotion of Post-Polio Patients. ASME Journal of Biomechanical Engineering 1996;118(3):405–411.

Ivanenko YP, Poppele RE, Lacquaniti F. Five Basic Muscle Activation Patterns Account for Muscle Activity During Human Locomotion. J Physiol 2004;556(Pt 1):267–282. [PubMed: 14724214]

Ivanenko YP, Poppele RE, Lacquaniti F. Spinal Cord Maps of Spatiotemporal Alpha-Motoneuron Activation in Humans Walking at Different Speeds. Journal of Neurophysiology 2006;95(2):602–618. [PubMed: 16282202]

Jansen BH, Miller VH, Mavrofrides DC, Jansen CWS. Multidimensional EMG Based Assessment of Walking Dynamics. IEEE Transactions on Neural Systems and Rehabilitation Engineering 2003;11 (3):294–300. [PubMed: 14518794]

Kang HG, Dingwell JB. A Direct Comparison of Local Dynamic Stability During Unperturbed Standing and Walking. Experimental Brain Research 2006;172(1):35–48.

Kang HG, Dingwell JB. Effects of Walking Speed, Strength and Range of Motion on Gait Stability in Healthy Older Adults. Journal of Biomechanics 2008a;41(14):2899–2905. [PubMed: 18790480]

Kang HG, Dingwell JB. Separating the Effects of Age and Walking Speed on Gait Variability. Gait and Posture 2008b;27(4):572–577. [PubMed: 17768055]

Kennel MB, Brown R, Abarbanel HDI. Determining Minimum Embedding Dimension Using a Geometrical Construction. Physical Review A 1992;45(6):3403–3411. [PubMed: 9907388]

Lin SI, Woollacott MH. Postural Muscle Responses Following Changing Balance Threats in Young, Stable Older, and Unstable Older Adults. Journal of Motor Behavior 2002;34(1):37–44. [PubMed: 11880248]

Nayfeh, AH.; Balachandran, B. Applied Nonlinear Dynamics: Analytical, Computational, and Experimental Methods. New York, New York: John Wiley & Sons; 1995z.

Neptune RR, Sasaki K, Kautz SA. The Effect of Walking Speed on Muscle Function and Mechanical Energetics. Gait and Posture. 2007

Niino N, Tsuzuku S, Ando F, Shimokata H. Frequencies and Circumstances of Falls in the National Institute for Longevity Sciences, Longitudinal Study of Aging (NILS-LSA). Journal of Epidemiology 2000;10(1 Suppl):S90–S94. [PubMed: 10835834]

Packard NH, Crutchfield JP, Farmer JD, Shaw RS. Geometry from a Time Series. Physical Review Letters 1980;45:712–716.

Pijnappels M, Bobbert MF, Dieën JHv. Control of Support Limb Muscles in Recovery after Tripping in Young and Older Subjects. Experimental Brain Research 2005;160(3):326–333.

Rosenstein MT, Collins JJ, DeLuca CJ. A Practical Method for Calculating Largest Lyapunov Exponents from Small Data Sets. Physica D: Nonlinear Phenomena 1993;65:117–134.

Shiavi R. Electromyographic Patterns in Adult Locomotion: A Comprehensive Review. Journal of Rehabilitation Research and Development 1985;22(3):85–98. [PubMed: 2940361]

Shiavi R, Bugle HJ, Limbird T. Electromyographic Gait Assessment, Part 1: Adult EMG Profiles and Walking Speed. Journal of Rehabilitation Research and Development 1987;24(2):13–23. [PubMed: 3585781]

Shik ML, Orlovsky GN. Neurophysiology of Locomotor Automatism. Physiological Reviews 1976;56 (3):465–501. [PubMed: 778867]

Strogatz, SH. Nonlinear Dynamics and Chaos: With Applications to Physics, Biology, Chemistry, and Engineering. Cambridge, Massachusetts: Perseus Group; 1994.

Winter DA, Yack HJ. EMG Profiles During Normal Human Walking: Stride-to-Stride and Inter-Subject Variability. Electroencephalography and Clinical Neurophysiology 1987;67(5):402–411. [PubMed: 2444408]
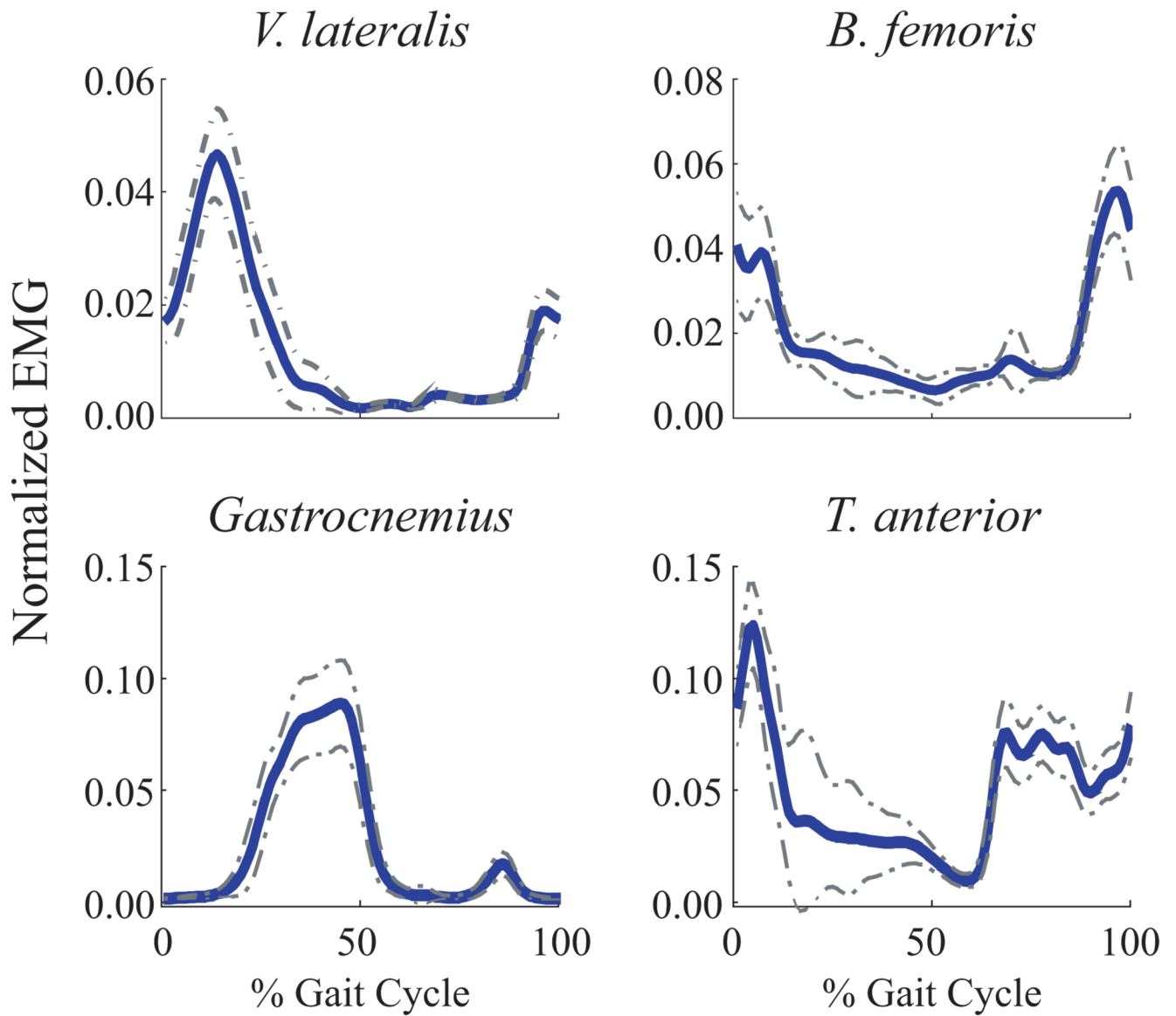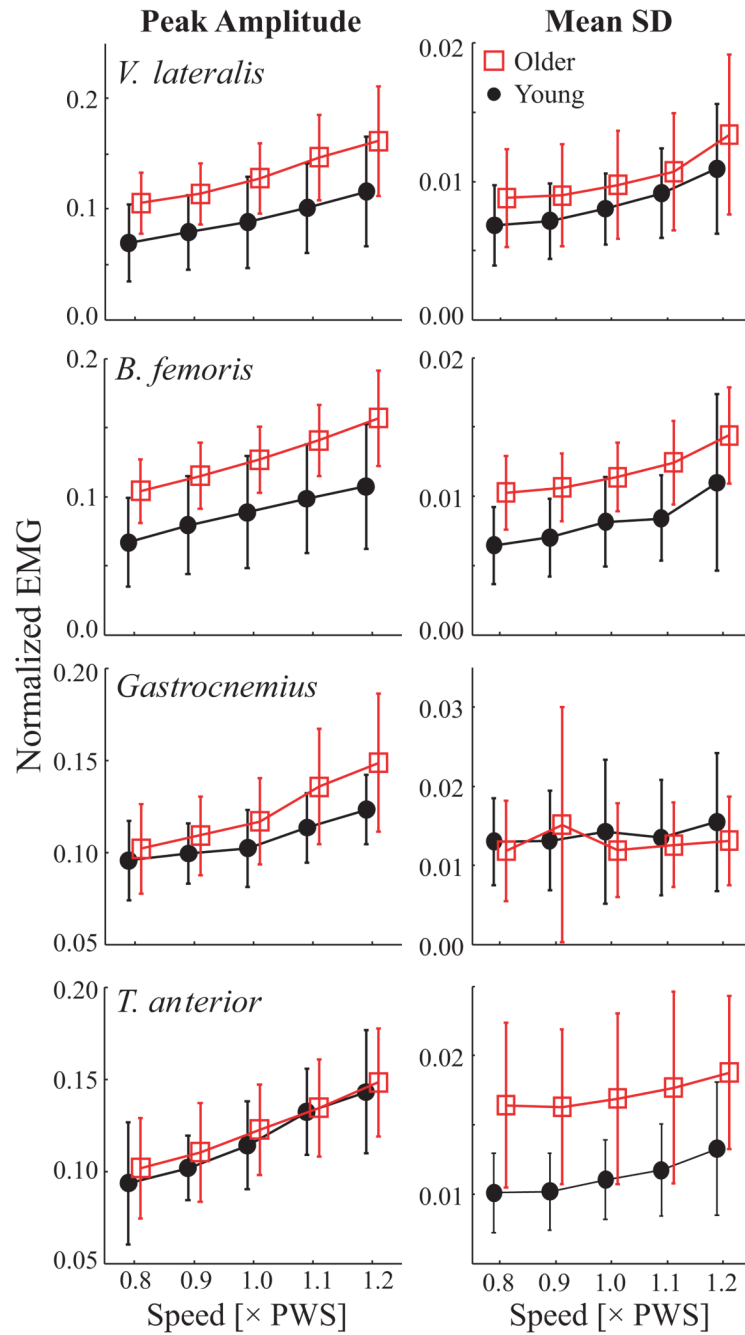
Figure 1.
Normalized (unitless) EMG Linear Envelopes from a single trial for a typical subject. The solid line represents the average and the dashed line represents ± 1 standard deviation (SD) across all strides within that trial. MeanSD was defined as the average thickness of the ± 1 SD band over the gait cycle.
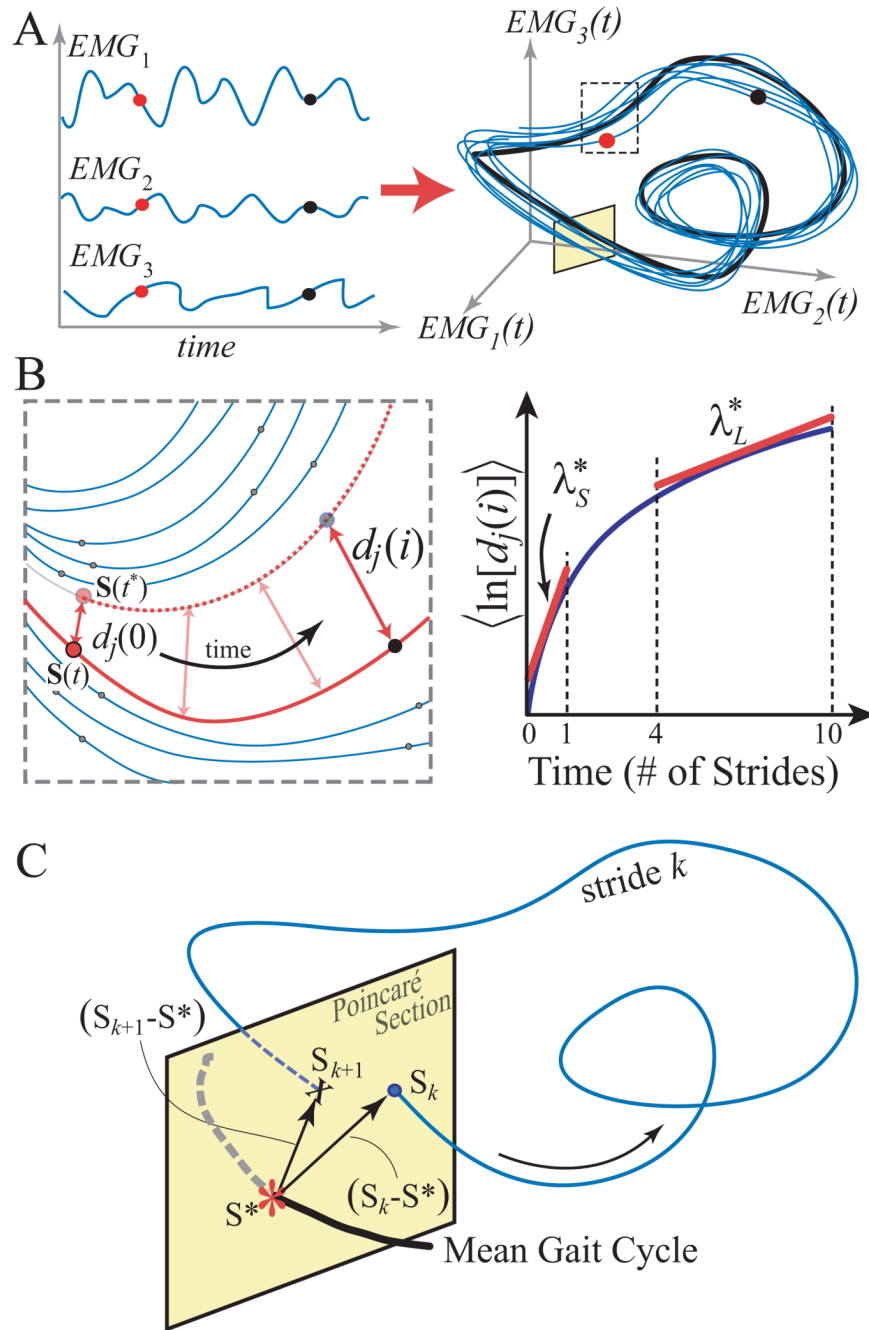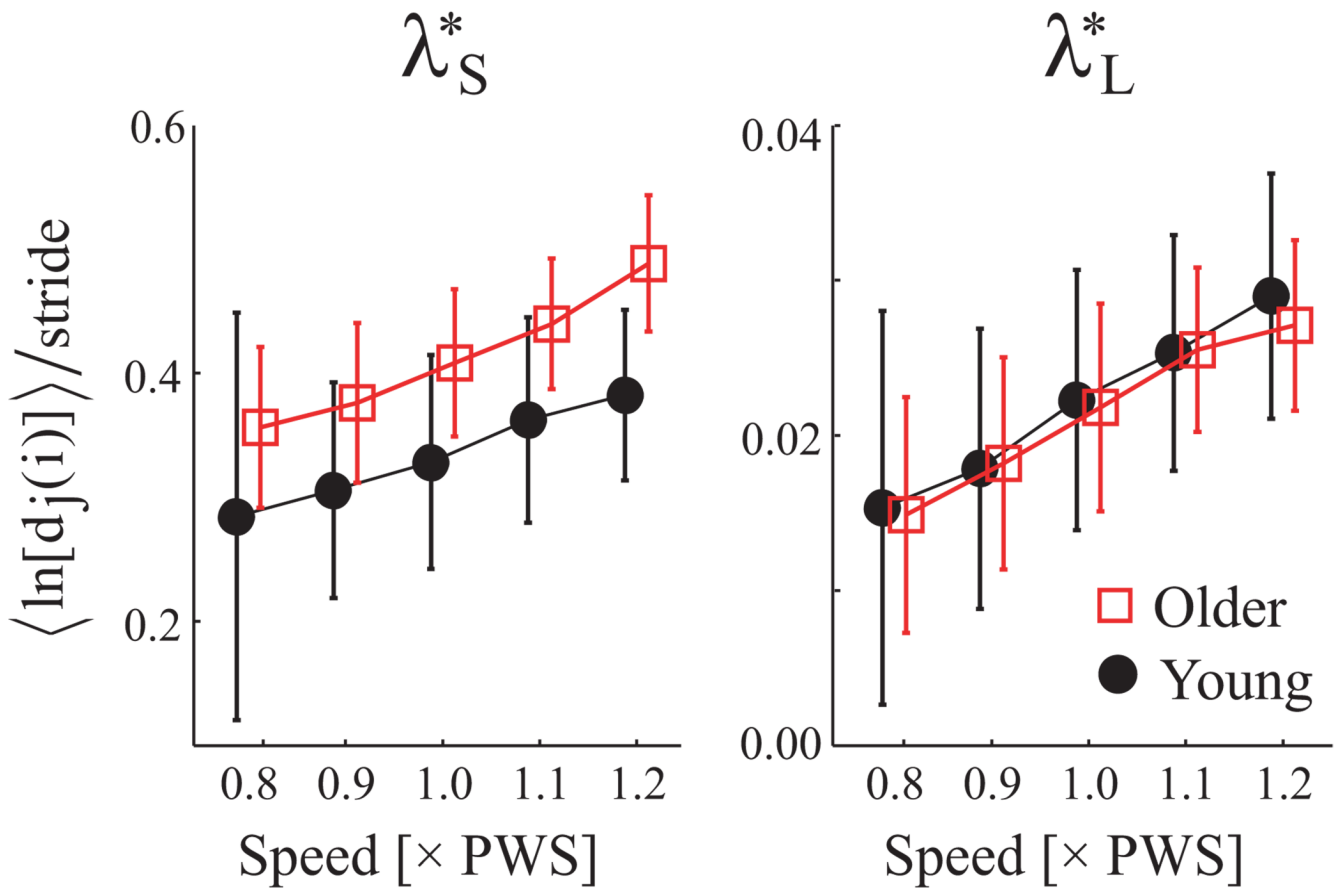
Figure 2.
Schematic representation of state space embedding and dynamic stability analyses of EMG signals. **A**: The original time series of each EMG signal and its derivative defined the states of the system (Eq. 2). These states were combined to form the system's trajectory in state space (only 3 states are shown here used for illustrative purposes). **B**: Expanded view of a typical local region. A small perturbation moves the system at $S(t)$ to its closest neighbor $S(t^*)$. Local divergence is computed by measuring the Euclidean distances between the subsequent points, denoted $d_j(i)$. The local dynamic stability is defined by how quickly, on average, the two trajectories diverge away from each other. Local rates of divergence, λ^*_S and λ^*_L, were calculated from the slopes of the mean log divergence curve (Eq. 3). **C**: Poincaré sections were

defined to be orthogonal to the mean (i.e., limit) cycle. The system state, S_k, at stride k evolves to S_{k+1} one stride later. Floquet multipliers quantify, on average, whether the distances between these states and the system fixed point, S^*, grow or decay after one cycle (Eq. 6).

Figure 3.
Peak amplitudes and MeanSD of normalized (unitless) EMG linear envelopes vs. Age and Speed. Error bars denote between-subject standard deviations within each group. **Left**: Between-strides average of EMG linear envelope peak amplitudes. Amplitudes increased with speed for all four muscles ($p < 0.001$). Older adults displayed higher amplitudes in *v. lateralis* ($p < 0.003$), *b. femoris* ($p < 0.001$), and *gastrocnemius* ($p < 0.03$). **Right**: MeanSD of EMG envelopes. EMG variability increased significantly with speed for *v. lateralis*, *b. femoris*, and *t. anterior* (all $p < 0.001$). Older adults exhibited significantly greater variability in *b. femoris* ($p = 0.003$) and *t. anterior* ($p < 0.001$).
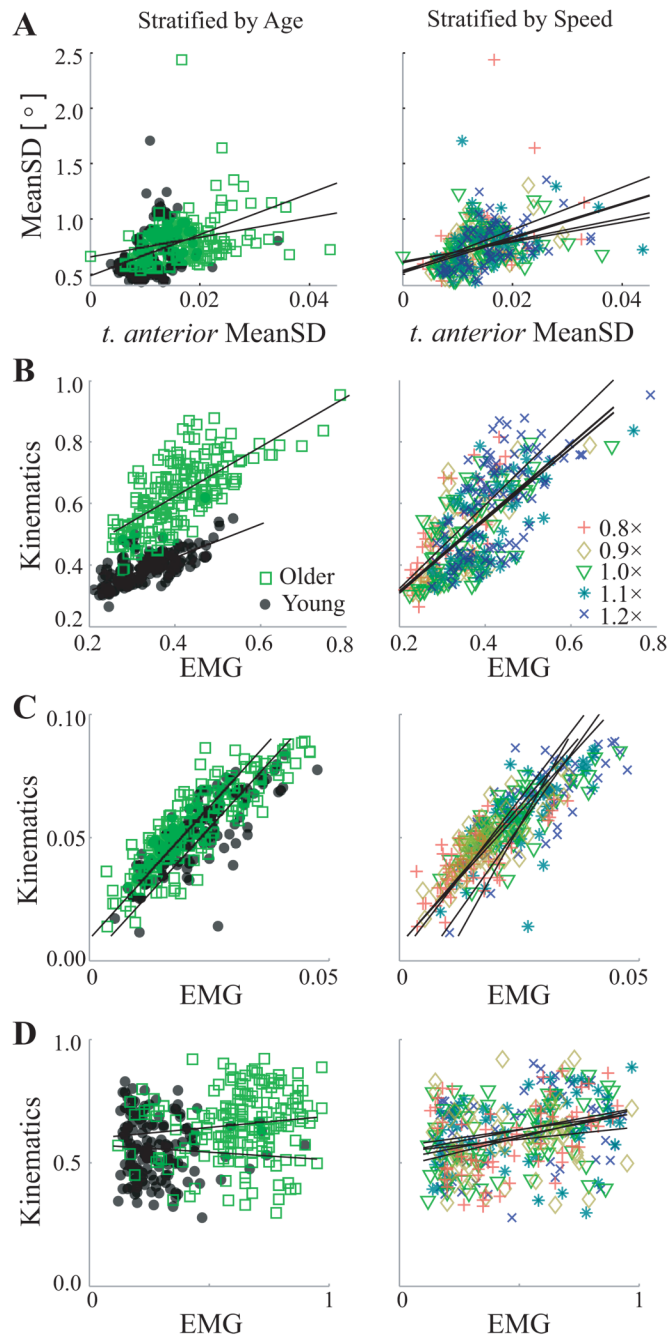
Figure 4.
Short-term (λ^*_S) and long-term (λ^*_L) local divergence exponents (units = 1/stride) vs. Age and Speed. Error bars denote between-subject standard deviations within each group. All subjects became locally more unstable with increased speed ($p < 0.001$). Older adults exhibited larger short-term (λ^*_s) exponents relative to young subjects ($p = 0.002$), but no differences for long-term (λ^*_L) exponents ($p = 0.980$).
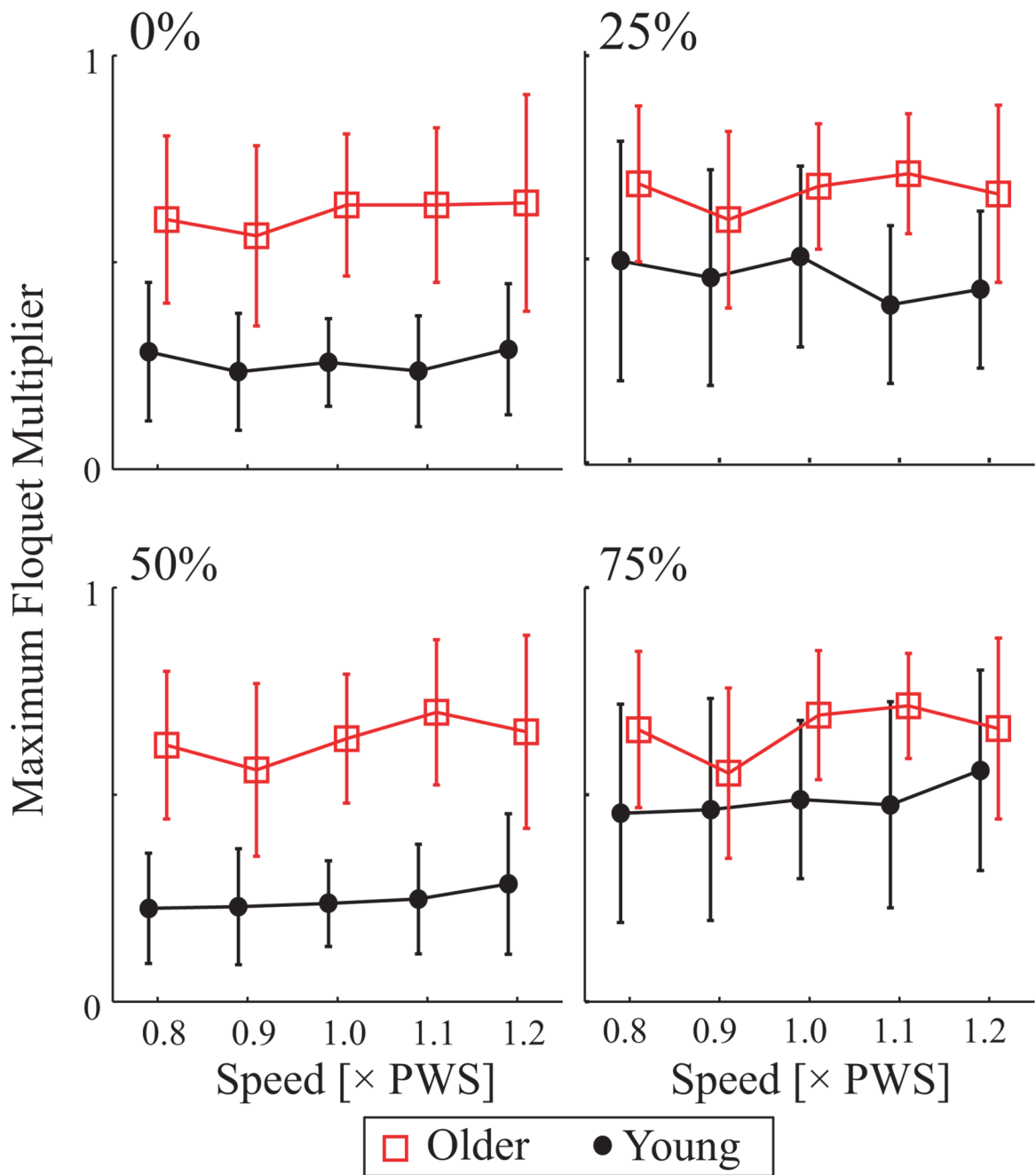
Figure 5.
Maximum Floquet Multipliers (FM; unitless) vs. Age and Speed for Poincaré sections taken at 0, 25, 50, and 75% of the gait cycle. Error bars denote between-subject standard deviations within each group. Older adults exhibited larger maximum FM values than Young adults ($p \leq 0.008$). Maximum FM did not vary with walking speed ($p \geq 0.170$). Qualitatively similar results were obtained for all Poincaré sections.

Figure 6.
Correlations between primary dependent measures, stratified by both Age (left) and Speed (right). **A**: Sagittal plane knee flexion/extension variability and *t. anterior* variability were slightly correlated after accounting for Age and Speed effects ($R^2 = 0.07$; $p < 0.001$). **B**: Short-term (λ^{*}_{s}) local divergence exponents derived from kinematics (Kang and Dingwell, 2008a) and EMG (Fig. 4) were strongly correlated ($R^2 = 0.38$; $p < 0.001$). **C**: Longterm (λ^{*}_{L}) local divergence exponents derived from EMG and kinematics were also strongly correlated ($R^2 = 0.52$; $p < 0.001$). **D**: Maximum FM derived from kinematics (Kang and Dingwell, 2008a) and EMG (Fig. 5) were not correlated after accounting for Age and Speed effects ($R^2 < 0.01$; $p = 0.41$).

Table 1

Subject Characteristics

	Young adults	Older Adults	p-value
Gender (M/F)	12/5[*]	12/6	0.55[**]
Age (years)	23.3 ± 2.6	72.1 ± 6.0	<0.0001
Height (m)	1.73 ± 0.094	1.70 ± 0.104	0.36
Body Mass (kg)	71.1 ± 9.86	73.2 ± 12.3	0.58
Preferred Walking Speed (PWS) (m/s)	1.30 ± 0.10	1.29 ± 0.15	0.86
PWS Range (m/s)	1.16 – 1.56	0.93 – 1.52	

[*] Reflects the number after the data for one young subject were discarded

[**] Fisher's Exact Test (χ^2)

Table 2

Effects of Age and Speed on EMG variability and dynamic stability (p-values)

		Age	Speed	Age × Speed
Interstride Variability	*v. lateralis*	0.18	<0.001	0.66
	b. femoris	0.003	<0.001	0.74
	gastrocnemius	0.407	0.027	0.54
	t. anterior	<0.001	<0.001	0.71
Local dynamic stability	λ^{*}_{S}	0.002	<0.001	0.76
	λ^{*}_{L}	0.98	<0.001	0.99
Orbital Stability	0%	<0.001	0.17	0.025
	25%	0.002	0.19	<0.001
	50%	<0.001	0.18	0.57
	75%	0.008	0.23	0.027